

Self-assembled Ni/TiO₂ nanocomposite anodes synthesized via electroless plating and atomic layer deposition on biological scaffolds

Konstantinos Gerasopoulos, Xilin Chen, James Culver, Chunsheng Wang and Reza Ghodssi

Supporting Information

Experimental Section

Preparation of Ni/TiO₂ composite anodes: Steel disks 15.5mm in diameter (Pred Materials International, USA) were coated using a table-top sputtering tool (Sputter coater 108, Ted Pella, Inc, USA) using a current of 2 mA for 50s. The substrates were then immersed in a phosphate buffer solution at pH 7 containing TMV1cys (the virus mutant used in this work) at a concentration of 1 gL⁻¹ purified as previously described and allowed to incubate for 1-2 days to maximize the virus attachment. After TMV self-assembly, the disks were immersed in a solution consisting of 10 mM sodium tetrachloropalladate (NaPdCl₄, 98 %, Sigma Aldrich, MO, USA) and phosphate buffer at a volume ratio of 1:12. This step takes place for approximately 2 hours and is followed by the nickel electroless plating reaction; the stock nickel solution (25 ml) was prepared by mixing 0.6 g nickel chloride (NiCl₂, 99%, Sigma Aldrich, MO, USA), 0.45 g glycine (tissue grade, Fischer Scientific, PA, USA), 1.5 g sodium tetraborate (Na₂B₄O₇, 99%, Sigma Aldrich, MO, USA) and 0.77 g dimethylamine borane (DMAB, 97%, Sigma Aldrich, MO, USA). This solution was mixed with DI water in a 1:1 ratio and chips were immersed in the bath for 3-5 minutes. Deposition of TiO₂ was performed in a BENEQ TFS 500 ALD reactor by alternate pulses of tetrakis-dimethyl amido titanium (TDMAT) and H₂O at 150°C as described previously.^[10] The deposition rate was 0.055 nm/cycle and 364 cycles (~2s/cycle) were used to achieve the desired thickness.

Structural characterization: SEM images were obtained using the steel disk samples with a Hitachi SU-70 FESEM. Powder pattern was recorded on a Bruker D8 Advance powder diffractometer equipped with LynxEye PSD detector and Ni β-filter using CuKα radiation from sealed tube. Measurement was performed in θ/θ mode from 10 to 100° 2θ and 015777° 2θ step with total exposition of 154 sec per point. TEM samples were prepared by mechanically removing the virus nanomaterials from the steel disk and dispersing them in ethanol solution. Droplets from the suspension were pipetted onto copper TEM grids. TEM images were obtained with a JEOL 2100 TEM/STEM machine while EDS spectra were collected with an Oxford INCA 250 system attached to the TEM tool.

Cell preparation and electrochemical characterization: The TiO₂ anodes were used as the working electrode in coin cells (R032) against a lithium metal foil (Sigma Aldrich, MO, USA) which was cut into a circular shape. The foil was attached to a steel surface and a Celgard separator (Celgard® 3501) was placed between the two electrodes. Five to six droplets of a 1M LiPF₆ solution in ethyl carbonate/diethylcarbonate (EC/DEC, 1:1, Novolyte Technologies, OH, USA) were used as the electrolyte. Cell assembly was

performed in a glove box with oxygen concentration of less than 0.1 ppm and Argon as the carrier gas. Galvanostatic experiments were performed using a multiple channel battery test station (Arbin Instruments, TX, USA) while cyclic voltammetry and electrochemical impedance spectroscopy data were collected using a Solartron 1287A Potentiostat with frequency analyzer (Hampshire, UK). The same equipment was used to obtain the rate capability data for the electrodes without TMV, since the current required at low rates could not be accurately provided by the Arbin instrument.

Structural Characterization

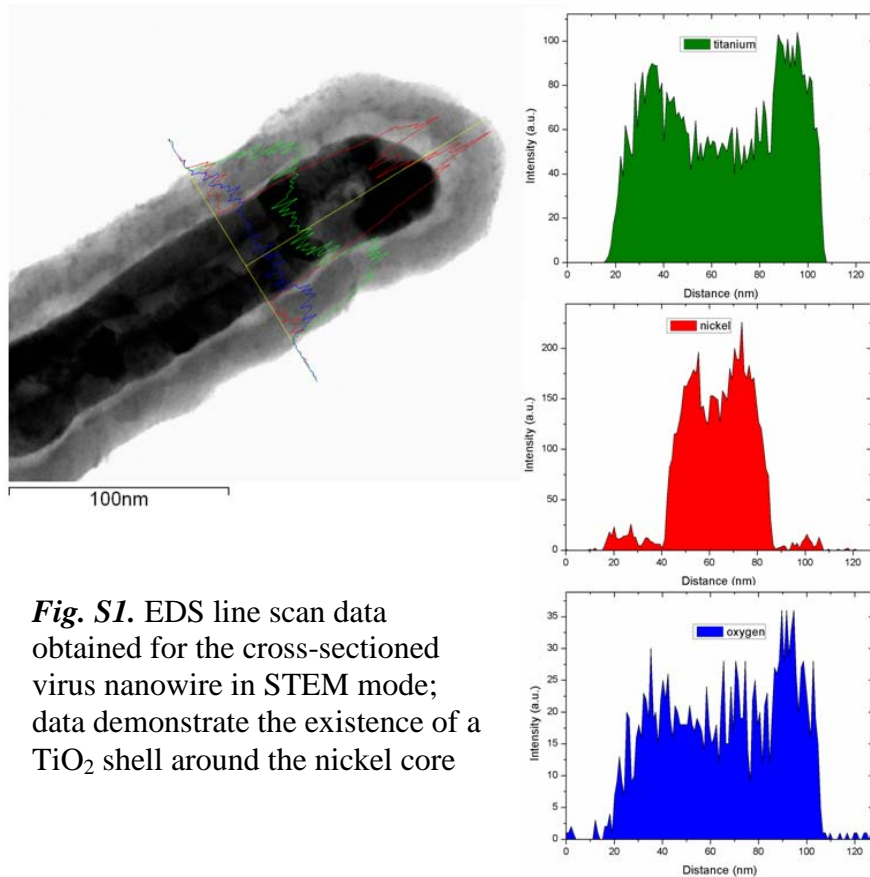


Fig. S1. EDS line scan data obtained for the cross-sectioned virus nanowire in STEM mode; data demonstrate the existence of a TiO_2 shell around the nickel core

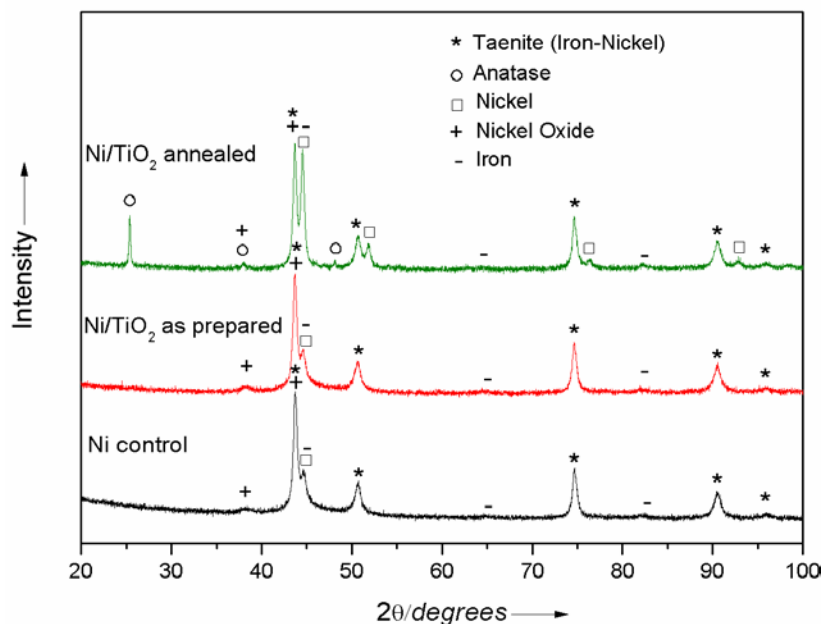


Fig. S2. XRD data for three samples: Ni-coated TMV only, Ni/TiO₂-coated TMV (as prepared), and Ni/TiO₂-coated TMV (annealed at 450°C). Peaks are identified for anatase, syn TiO₂ (JCPDS 78-2486), taenite, syn Iron-Nickel (JCPDS 47-1417), nickel, syn Ni (JCPDS 04-0850), nickel oxide, syn NiO (JCPDS 78-0643), iron, syn Fe (JCPDS 06-0696). The anatase peaks are found only in the annealed sample.

Electrochemical Characterization

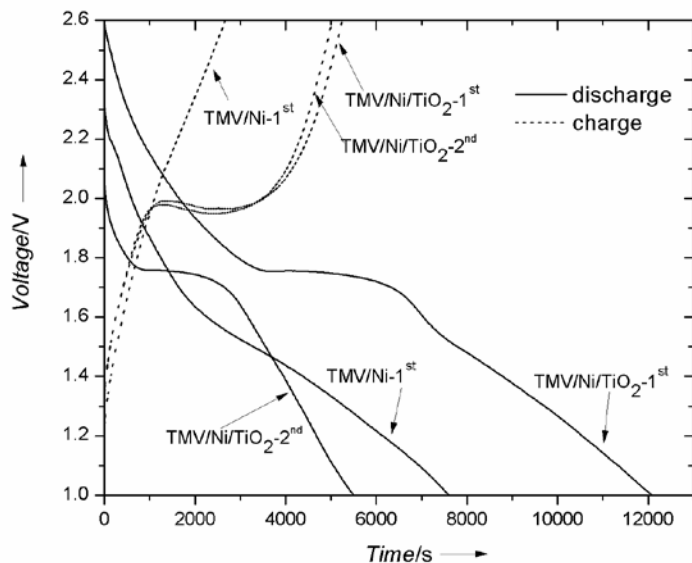


Fig. S3. Graph showing the 1st and 2nd charge/discharge curves for the nanostructured TMV/Ni/TiO₂ electrodes as well as the 1st cycle for a control sample without the TiO₂ layer (TMV/Ni). The samples were cycled at the same current value and the x-axis is given in a time scale since the exact loading of the nickel-coated TMV is not known. The large irreversible capacity for the TiO₂-containing anode in the first cycle can be attributed to conversion of some NiO to Ni in the underlying layer core (see TMV/Ni curve-1st). As shown in the figure, this process is highly irreversible. As a result, the capacity of the nanocomposite TMV/Ni/TiO₂ can be fully recovered after the 2nd cycle.

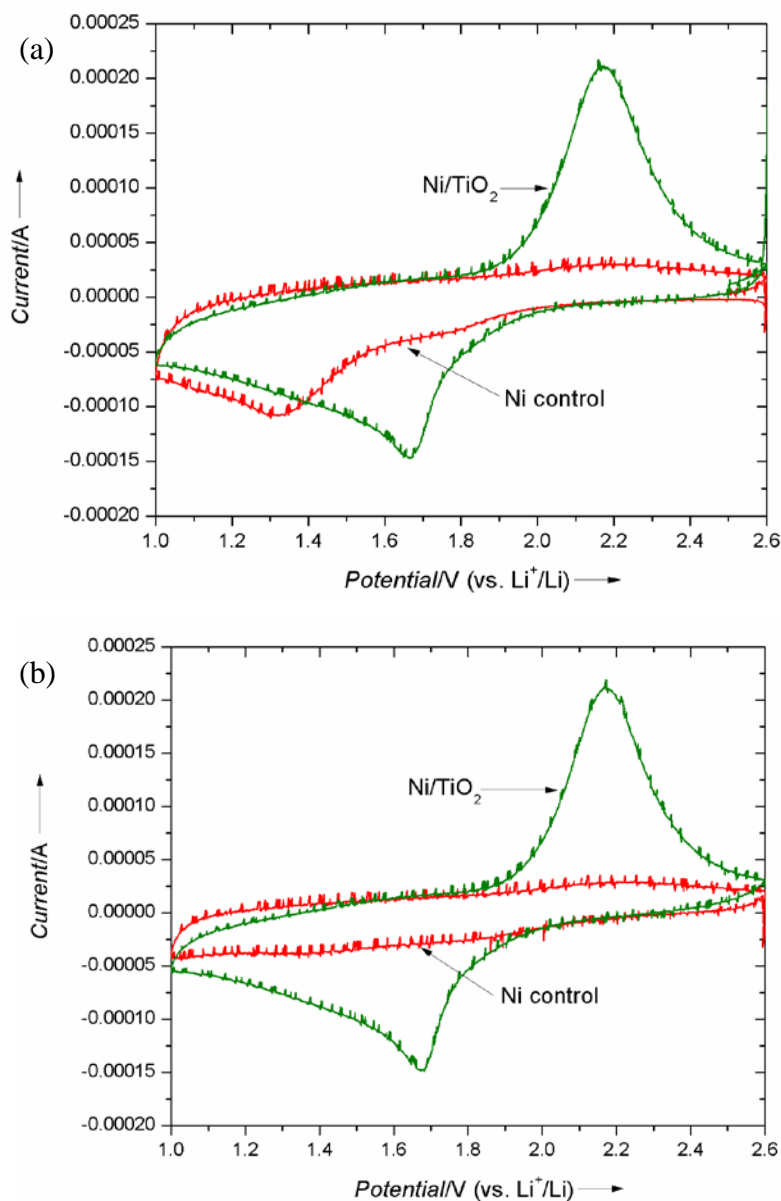


Fig. S4. CV scans for the first (a) and second (b) cycles for the synthesized TMV/Ni/TiO₂ nanocomposite anode (green) and a control sample without the TiO₂ layer (TMV/Ni, red) obtained in the range of 1-2.6 V at a rate of 0.5 mVs⁻¹; Figure S4a indicates that there is an insertion peak for the control sample, corresponding to some NiO that is present in the core of the nanocomposite. The extraction peak is not observed for the control sample and both peaks have vanished in the second cycle (figure S4b).

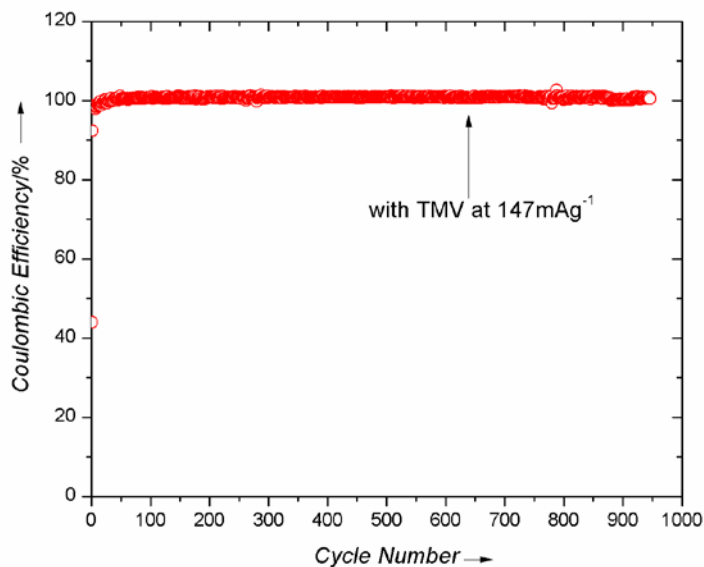


Fig. S5. Coulombic efficiency (charge capacity/discharge capacity) in % for the TMV/Ni/TiO₂ sample cycled at 147 mA g⁻¹. The efficiency during the 1st, 2nd and 3rd cycles is 44%, 92.3% and 98% respectively and stabilizes to values higher than 99.5% by the 13th cycle indicating the excellent reversibility of the lithium insertion process into the TiO₂ structure.

Post-Testing Characterization

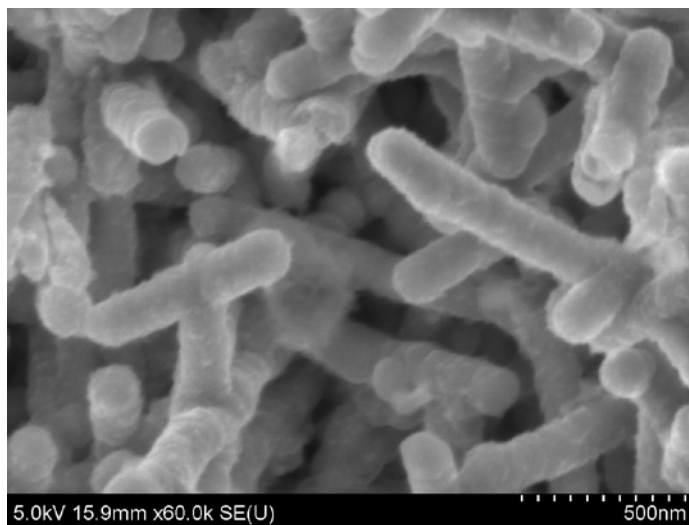


Fig. S6. SEM image of the nanostructured anode that was cycled at the 500 mA g⁻¹ rate after completion of approximately 850 cycles. Before disassembly, the cell was kept at 2.6 V for 48 hours to ensure removal of all lithium from the structure. **It is observed that the virus nanomaterials maintain their three-dimensional structure.**

Charge transfer kinetics

The kinetics of the lithium reaction in the electrodes were investigated using Electrochemical Impedance Spectroscopy (EIS). EIS data were collected at the open circuit potential before cycling experiments at 150 mA g^{-1} as well as after the 12th cycle when the capacity has stabilized for the TMV-coated anode. The second set of data was obtained after lithium insertion (i.e. after discharge). An AC signal of 10 mV in amplitude was applied and the frequency was swept from 1 MHz to 5 mHz. The results are demonstrated in Fig.S7. There is only one semicircle in the high frequency region (small Z' values) corresponding to the charge transfer resistance while the low frequency region is controlled by lithium ion diffusion. In the case of the nanostructured TiO_2 , however, the semicircle is much smaller both before testing as well as after 12 cycles, indicating a smaller charge transfer resistance in this electrode. The improved reaction kinetics enabled by the viral template provide further explanation for the superior cycling performance as well as the high rate capability.

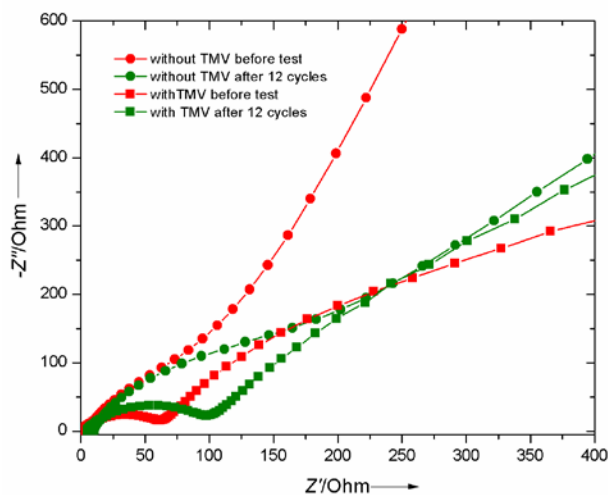


Fig. S7. EIS data for electrodes with and without TMV cycled at 150 mA g^{-1} . The data were collected at open circuit potential before cycling and after the 12th discharge.